7-2014

Investigation of ferroelectric domains in thin films of vinylidene fluoride oligomers

Pankaj Sharma
University of Nebraska at Lincoln, psharma@huskers.unl.edu

Shashi Poddar
University of Nebraska-Lincoln, shashi.poddar@huskers.unl.edu

Rafal Korlacki
University of Nebraska-Lincoln, rkorlacki2@unl.edu

Stephen Ducharme
University of Nebraska-Lincoln, sducharme1@unl.edu

Alexei Gruverman
University of Nebraska-Lincoln, agruverman2@unl.edu

Investigation of ferroelectric domains in thin films of vinylidene fluoride oligomers

Pankaj Sharma,[1,a)] Shashi Poddar,[1] Rafal Korlacki,[2] Stephen Ducharme,[1] and Alexei Gruverman[1,b)]
[1]*Department of Physics and Astronomy, and Nebraska Center for Materials and Nanoscience, University of Nebraska-Lincoln, Nebraska 68588, USA*
[2]*Department of Electrical Engineering and Center for Nanohybrid Functional Materials, University of Nebraska-Lincoln, Nebraska 68588, USA*

(Received 18 April 2014; accepted 4 July 2014; published online 15 July 2014)

High-resolution vector piezoresponse force microscopy (PFM) has been used to investigate ferroelectric domains in thin vinylidene fluoride oligomer films fabricated by the Langmuir-Blodgett deposition technique. Molecular chains are found to be preferentially oriented normal to the substrate, and PFM imaging shows that the films are in ferroelectric *β-phase* with a predominantly in-plane polarization, in agreement with infrared spectroscopic ellipsometry and X-ray diffraction measurements. The fractal analysis of domain structure has yielded the Hausdorff dimension (D) in the range of ∼1.3–1.5 indicating a random-bond nature of the disorder potential, with domain size exhibiting Landau-Lifshitz-Kittel scaling. © *2014 AIP Publishing LLC*.
[http://dx.doi.org/10.1063/1.4890412]

Polyvinylidene fluoride (PVDF) based ferroelectric materials have been a focus of continuous research activities[1–5] since the discovery of piezo-,[6–8] pyro-,[9,10] and ferroelectricity[11–14] in these fluorinated polymers. In particular, VDF oligomers, which contain a finite number (n) of VDF units, present a unique opportunity to not only fabricate highly ordered crystalline ultra-thin films, but also control their functional properties by varying the orientation and length of molecular chains.[15,16] The finite-length VDF oligomers appear to be functionally equivalent to PVDF but display better crystallinity and improved ferroelectric properties.[17] Furthermore, oligomers are amenable to a wider range growth and fabrication methods including epitaxial growth.[14] Structurally, VDF oligomers have different possible terminal functional groups ($Q = CH_3$, CF_3; $R = OH$, I, etc.) at the ends of the molecular chains: Q-$[CH_2$-$CF_2]_n$-R (Fig. 1).

Investigation of static domain arrangement along with their dynamic and scaling behavior is critical both from a fundamental and technological viewpoints as many functional properties of ferroelectric materials are determined by interplay and transformation between equivalent energy (polarization) states. Yet, there are no studies of ferroelectric domains and their scaling in VDF oligomer films. In this article, using high-resolution vector piezoresponse force microscopy (vector-PFM),[18,19] we have investigated ferroelectric domain structure in as-grown thin films of VDF oligomers fabricated by Langmuir-Blodgett (LB) deposition with the thickness ranging from approximately 4.4 nm up to 150 nm. It has been found that the molecular chains tend to preferentially align normal to the substrate as the increasing number of layers is being deposited in succession. PFM imaging shows that the as-grown VDF oligomer films are in ferroelectric *β-phase* with a predominantly in-plane polarization. Fractal analysis of irregular as-grown domain arrangement yields a Hausdorff dimension (D) in the range of ∼1.3–1.5, and average domain size scales according to the well-known Landau-Lifshitz-Kittel (LLK) scaling law.[20–22]

The oligomer for the present study had the composition CF_3-$[CH_2$–$CF_2]_n$–I, where $n = 17 \pm 2$ was obtained from Kunshun Hisense and used as received. The oligomer powder was dissolved in dimethylsulfoxide (DMSO) to a concentration of 0.05% by weight and dispersed on the LB trough, compressed to a surface pressure of 5 mN/m and transferred by horizontal contact one layer (monolayer—ML) at a time to a highly doped silicon substrate. The deposition process is described in greater detail in Refs. 16 and 23. Previous studies have shown that under the same deposition conditions,

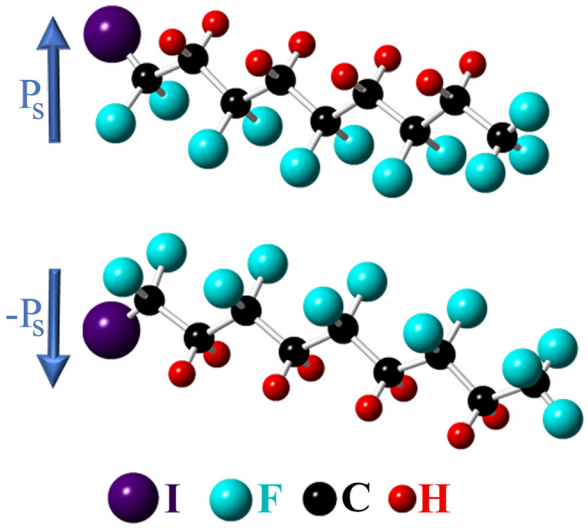

FIG. 1. Ball-and-stick model of Iodine (I) and CF_3 terminated VDF (CF_3-$\{CH_2$-$CF_2\}_4$-I) oligomer molecules with opposite directions of dipole moments.

a)psharma@huskers.unl.edu
b)alexei_gruverman@unl.edu

the oligomers are nearly perpendicular to the substrate, with the iodine toward the substrate, and form one monomolecular layer per transfer.[16,24] No subsequent (thermal/mechanical/electrical) treatment was applied to the samples after the LB deposition process. A commercial atomic force microscope (Asylum MFP-3D) was used in this study to visualize the ferroelectric domain structure. Vector PFM imaging has been performed using an AC bias with amplitude of 1 V and frequency in the 200–500 kHz range. Conductive Cr/Au-coated ($k = 0.09$ N/m, $R \sim 42$ nm) cantilevers of a triangular shape[25] have been used to achieve effective deconvolution of orthogonally oriented (two in-plane and one out-of-plane) polarization components. The thickness (d) of the samples has been determined either by cross-section profile analysis of the topographic images (for relatively thin samples, $d < 10$ nm) or by using ellipsometry analysis (for relatively thicker samples, $d > 15$–20 nm).

Figure 2 shows typical morphology of the VDF oligomer thin films with non-uniform substrate coverage. Cross-section analysis of 1-ML-thick film (Figs. 2(a) and 2(b)) yielded a film thickness of approximately 4.4 nm, which agrees well with the estimated VDF molecular chain length ($n \sim 18$ times the intra-chain periodicity distance, or VDF unit size, of 2.56 Å (Refs. 26 and 27)). This value also points out to the fact that the –*C*-*C*– chains in VDF films are aligned vertically on the Si substrate in agreement with our earlier infrared (IR) spectroscopic ellipsometry data[16] and are further supported by the X-ray diffraction measurements[28] (see Figs. S1–S3). The IR absorption spectra[28] (Fig. S1) are also consistent with the β-phase of the VDF. Vertical alignment of the molecular chains in the oligomer films is in contrast to PVDF and PVDF-TrFE (TrFE: Trifluoroethylene) films prepared by LB[23] or spin-cast methods,[29] and even epitaxial VDF oligomer films prepared by vacuum thermal evaporation[14] or solvent casting,[17] where the –*C*-*C*– chains preferably align parallel to the substrate. Moreover, a small spread in the measured chain length (standard deviation = 0.5 nm, inset Fig. 2(b)) over a relatively large area (~several μm^2) is well within the oligomer chain length ($\Delta n = \pm 2$) dispersion and besides could arise because of a small tilting of the –*C*-*C*– chains away from the substrate normal. In addition, stacking of the monolayers,[15] as a result of multiple LB transfers has been observed.[15,16] This is highlighted by detection of distinct morphological steps with a height of approximately 4.4 nm in the 3-ML-thick sample (Figs. 2(c) and 2(d)). In thicker samples, the stacking of the layers is not perfect due to non-uniform coverage of the substrate, and in this case, ellipsometry measurements have been used to determine the average film thickness.

To obtain detailed information about spatial arrangement of polarization, both in-plane and out-of-plane polarization components have been detected using lateral and vertical PFM modes (LPFM and VPFM, respectively).[30] Figures 3 and 4 show the spatial distribution of in-plane and out-of-plane polarization components in 1-ML-thick (~4.4 nm) and 8-ML-thick (~35 nm) samples. As can be seen in Figs. 3(d) and 4(d), the as-grown films are in a polydomain state with an average in-plane domain size of about 45 nm and 98 nm for the 1-ML-thick and 8-ML-thick films, respectively. The average domain sizes have been estimated by means of autocorrelation analysis described in detail in Ref. 31. Note that the spatial arrangement of the out-of-plane polarization is governed in general by electrical (i.e., screening in ambient, usually through adsorption of molecules, ions, etc.) and mechanical boundary conditions. For thin films (1 ML), where the screening is less efficient, formation of the antiparallel domains (Figs. 3(a) and 3(b)) with out-of-plane polarization component is a way for the system to reduce its free energy. For slightly thicker films (8 ML), the screening of the depolarizing field is more efficient and interaction with the substrate becomes a dominating factor resulting in a more uniform

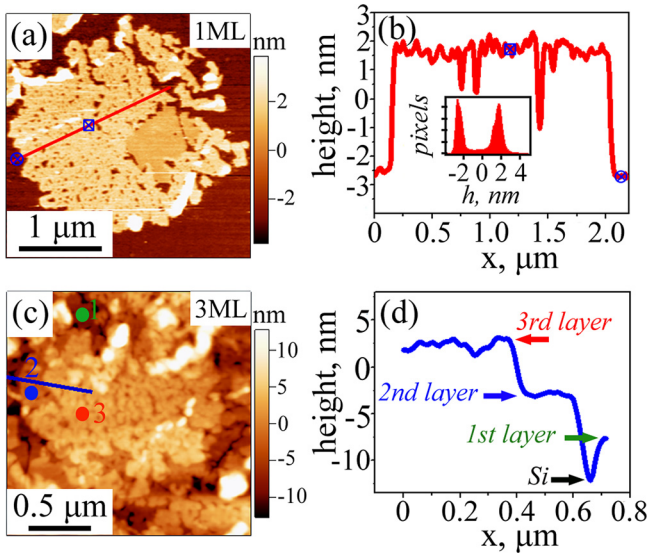

FIG. 2. (a) Topographic image of the 1-ML-thick VDF oligomer sample. (b) Cross-section of the height profile along the red line shown in (a). Inset in (b) shows the histogram of the height data for image (a). (c) Topographic image of the 3-ML-thick sample. (d) Cross-section of the height profile along the blue line shown in (c). In (c), dots indicate the stacking of the layers: green dot—1st layer, blue dot—2nd layer, and red dot—3rd layer.

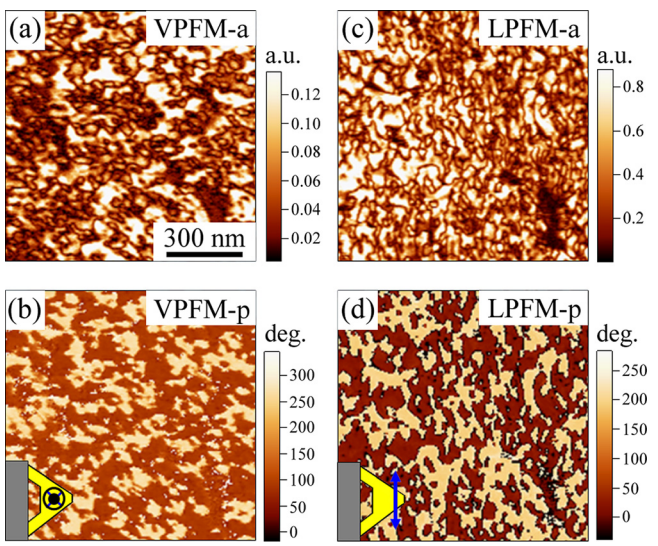

FIG. 3. Mapping of out-of-plane and in-plane polarization components in 1-ML sample: (a) and (b) VPFM amplitude (a), and phase (b) images, respectively. (c) and (d) Corresponding LPFM amplitude (c), and phase (d) images, respectively. In (b) and (d), the labels on the cantilever motifs indicate the direction of sensed polarization in the respective imaging modes.

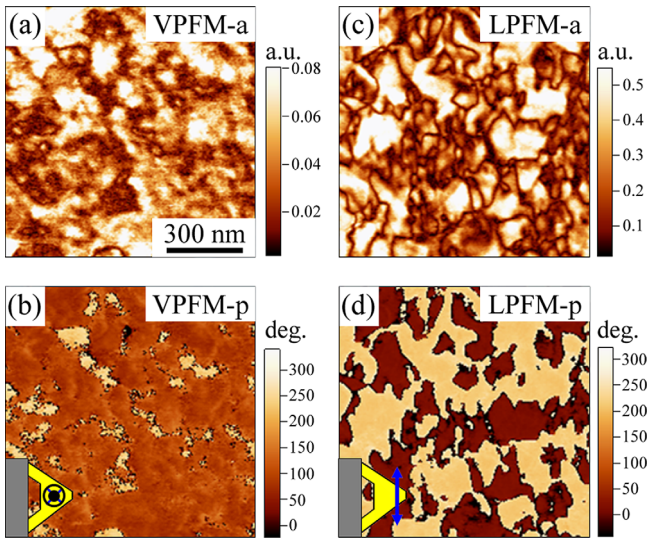

FIG. 4. Mapping of out-of-plane and in-plane polarization components in 8-ML sample: (a) and (b) VPFM amplitude (a), and phase (b) images, respectively. (c) and (d) Corresponding LPFM amplitude (c), and phase (d) images, respectively. In (b) and (d), the labels on the cantilever motifs indicate the direction of sensed polarization in the respective imaging modes.

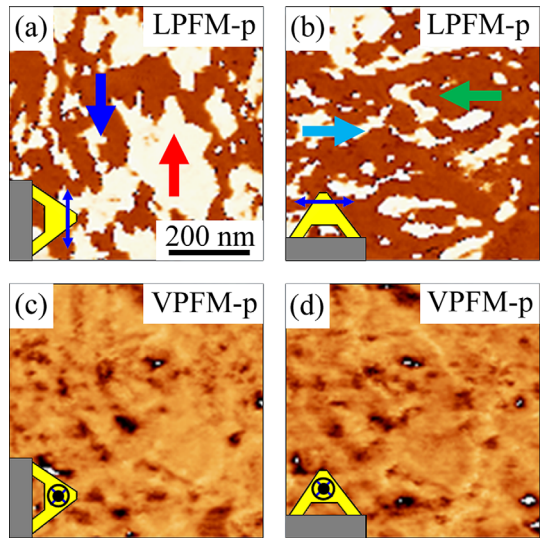

FIG. 5. Vector PFM mapping on a 5-ML-thick (~22 nm) VDF film: (a) and (b) LPFM phase images before (a), and after (b) rotation of sample by 90°. (c) and (d) VPFM phase images at the same location before (c), and after (d) rotation of the sample by 90°. In (a)–(d), the labels on the cantilever motifs indicate the direction of detected polarization in the respective imaging modes.

(mono-domain, Figs. 4(a) and 4(b)) out-of-plane polarization. Moreover, LPFM amplitude images (Figs. 3(c) and 4(c)) exhibit a nearly saturated signal in contrast to a rather low signal in VPFM amplitude images (the LPFM amplitude is about 10 times larger than the VPFM amplitude). Therefore, from these maps the following conclusion can be drawn: as-grown films are in a highly textured ferroelectric *β-phase*[28] (Figs. S1–S6, with details on AFM-tip induced switching in supplementary material Sec. III) with molecular chains oriented (nearly) normal to the substrate, exhibiting a predominantly in-plane polarization. In fact, a slight inclination of the –*C*-*C*– chains away from the substrate normal can explain a low VPFM response observed in Figs. 3(a) and 4(a). In case of PFM imaging using a rectangular cantilever, an additional contribution to the observed VPFM response[28] (see Fig. S7) can arise from cantilever *buckling*[32,33] as opposed to true *out-of-plane deflection*.

To unambiguously map out all polarization components (two in-plane and one out-of-plane), a vector-PFM approach has been used.[19] Figures 5(a) and 5(b) show PFM images of the orthogonal in-plane polarization components. VPFM images (Figs. 5(c) and 5(d)) show a nearly single-domain state for the out-of-plane polarization in contrast to the poly-domain state (with a high amplitude) for two in-plane components of the polarization (which suggests the existence of stable charged domain walls), in agreement with Figs. 3 and 4. Note that the VPFM images remain the same before and after the 90° rotation of the sample. This indicates an effective deconvolution of the VPFM and LPFM images, which therefore, represent a true (free from artifacts) spatial distribution of polarization in the VDF oligomer films.

The average size of domains w with in-plane polarization increases with increasing film thickness d following the well-known LLK scaling law: $w \sim kd^{1/2}$ (Fig. 6), where k describes a balance between the domain wall and electrostatic energies. This is despite the fact that LLK law was proposed initially for ferromagnetic materials,[20–22] and later extended to ferroelectric materials (exhibiting the same scaling)[34–36] with out-of-plane polar axis. Geometrical aspects of profoundly irregular in-plane domains have been studied by performing fractal analysis on the static domain patterns. The fractal dimension D has been determined from the log-log plot of the domain perimeter P versus domain area S using the WSxM software.[37] A value of D in the 1.3–1.5 range has been obtained. The fractal dimension can be viewed as the degree of roughness of a boundary between two phases (with 1 corresponding to a smooth curve with a continuous derivative and 2 to a very rough surface filling curve). The observed fractal-like domains (meandering of domain walls) reflect a dominance of the disorder potential,[38] which modifies the local internal potential landscape and governs the formation of thermodynamically stable static domain patterns over the elasticity effects. The obtained value of D is comparable to that reported for nanostructures of PVDF-TrFE LB films[39,40] and suggests a

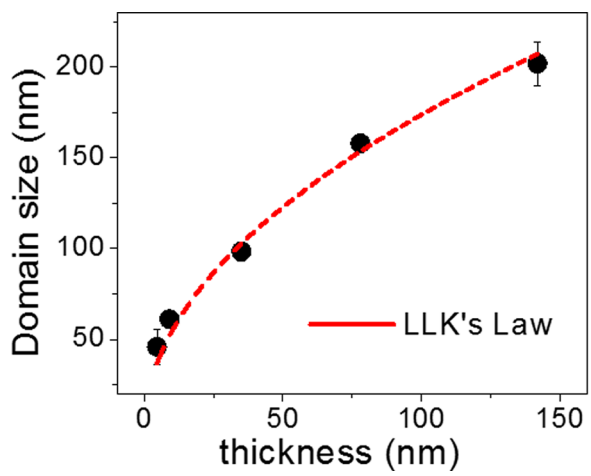

FIG. 6. Plot of average domain size vs thickness. Dotted red line represents domain-size scaling according to LLK law.

similar nature of the disorder potential, i.e., random-bond regime.

In summary, fractal-like domains in as-grown VDF oligomer films prepared by LB deposition were characterized by means of high-resolution vector PFM. It was shown that the *–C-C–* molecular chains of a finite length tended to align nearly normal to the film in stacks as the increasing number of layers is being deposited. The combined PFM and IR spectroscopic measurements showed that the films as thin as 4.4 nm were in the ferroelectric β-phase with a predominantly in-plane polarization. Landau-Lifshitz-Kittel domain scaling was observed for irregularly shaped ferroelectric domains having a fractal dimensionality $\sim$1.3–1.5 indicating a random-bond regime of the disorder potential. These findings will be useful for further studies of switching behavior of oligomer films and evaluation of their potential for electronic applications.

This research was supported by the U.S. Department of Energy, Office of Basic Energy Sciences, Division of Materials Sciences and Engineering under Award No. DE-SC0004530, by the National Science Foundation (Grant Nos. MRSEC DMR-0820521 and ECCS-1101256), and by the Nebraska EPSCoR Trans-disciplinary, Multi-Institutional Research Clusters Program. The mid-infrared ellipsometry measurements were performed at the Center for Nanohybrid Functional Materials core facility supported by the National Science Foundation under Award No. EPS-1004094. Authors thank Dr. Shah Valloppilly for his help with XRD measurements and Dr. Nina Hong of J.A. Woollam Co for her help with ellipsometry measurements of the VDF films. Authors thank Professor Serge Nakhmanson for his help with preparation of the ball-and-stick model of the VDF oligomer molecules.

[1]H. S. Nalwa, J. Macromol Sci. Rev. Macromol. Chem. Phys. **C31**, 341 (1991).
[2]L. E. Cross, Mater. Chem. Phys. **43**, 108 (1996).
[3]V. V. Kochervinskii, Russ. Chem. Rev. **68**, 821 (1999).
[4]L. M. Blinov, V. M. Fridkin, S. P. Palto, A. V. Bune, P. A. Dowben, and S. Ducharme, Physics-Uspekhi **43**(3), 243 (2000).
[5]K. Matsushige and H. Yamada, Ann. N. Y. Acad. Sci. **960**, 1 (2002).
[6]H. Kawai, Jpn. J. Appl. Phys., Part 1 **8**, 975 (1969).
[7]E. Fukuda, Phase Transitions **18**, 135 (1989).
[8]H. Kawai, Oyobuturi **39**, 413 (1970).
[9]E. Yamaka, T. Hayashi, M. Matsumoto, N. Murayama, and H. Hashizume, Autumn meeting of Jpn. Soc. Appl. Phys. **32**, 292 (1971).
[10]J. G. Bergman, J. H. MaFee, and G. R. Crane, Appl. Phys. Lett. **18**, 203 (1971).
[11]T. Furukawa, M. Date, and E. Fukada, J. Appl. Phys. **51**, 1135 (1980).
[12]T. Yagi, M. Tatemoto, and J. Sako, Polym. J. **12**, 209 (1980).
[13]T. Furukawa, G. E. Johnson, and H. E. Bair, Ferroelectrics **32**, 61 (1981).
[14]K. Noda, K. Ishida, A. Kubono, T. Horiuchi, H. Yamada, and K. Matsushige, Jpn. J. Appl. Phys., Part 1 **39**, 6358 (2000).
[15]S. Kuwajima, S. Horie, T. Horiuchi, H. Yamada, K. Matsushige, and K. Ishida, Macromolecules **42**, 3353 (2009).
[16]R. Korlacki, J. T. Johnson, J. Kim, S. Ducharme, D. W. Thompson, V. M. Fridkin, Z. Ge, and J. M. Takacs, J. Chem. Phys. **129**, 064704 (2008).
[17]S. Chen, K. Yao, and F. E. H. Tay, Polym. Int. **61**, 169 (2012).
[18]E. Soergel, J. Phys. D: Appl. Phys. **44**, 464003 (2011).
[19]S. V. Kalinin, B. J. Rodriguez, S. Jesse, J. Shin, A. P. Baddorf, P. Gupta, H. Jain, D. B. Williams, and A. Gruverman, Microsc. Microanal. **12**, 206 (2006).
[20]L. Landau and E. Lifshitz, Phys. Z. Sowjetunion **8**, 153 (1935).
[21]C. Kittel, Phys. Rev. **70**, 965 (1946).
[22]C. Kittel, Rev. Mod. Phys. **21**, 541 (1949).
[23]S. Ducharme, S. P. Palto, and V. M. Fridkin, in *Handbook of Thin Film Materials*, edited by H. S. Nalwa (Academic Press, San Diego, 2002), Vol. 3.
[24]S. M. Nakhmanson, R. Korlacki, J. T. Johnston, S. Ducharme, Z. X. Ge, and J. M. Takacs, Phys. Rev. B **81**, 174120 (2010).
[25]I. Chasiotis, in *Springer Handbook of Experimental Solid Mechanics*, edited by William N. Sharpe, Jr. (Springer, Boston, 2008).
[26]K. Noda, K. Ishida, T. Horiuchi, K. Matsushige, and A. Kubono, J. Appl. Phys. **86**, 3688 (1999).
[27]M. Kobayashi, K. Tashiro, and H. Tadokoro, Macromolecules **8**, 158 (1975).
[28]See supplementary material at http://dx.doi.org/10.1063/1.4890412 for more experimental details on Mid-Infrared (IR) spectroscopic ellipsometry, XRD, PFM, and AFM-tip induced switching measurements.
[29]T. Furukawa, Y. Takahashi, and T. Nakajima, Curr. Appl. Phys. **10**, e62 (2010).
[30]A. Gruverman and S. V. Kalinin, J. Mater. Sci. **41**, 107 (2006).
[31]P. Sharma, T. Reece, D. Wu, V. M. Fridkin, S. Ducharme, and A. Gruverman, J. Phys. Condens. Matter **21**, 485902 (2009).
[32]C. Harnagea, M. Vallieres, C. P. Pfeffer, D. Wu, B. R. Olsen, A. Pignolet, F. Legare, and A. Gruverman, Biophys. J. **98**, 3070 (2010).
[33]P. Sharma, D. Wu, S. Poddar, T. J. Reece, S. Ducharme, and A. Gruverman, J. Appl. Phys. **110**, 052010 (2011).
[34]T. Mitsui and J. Furuichi, Phys. Rev. **90**, 193 (1953).
[35]J. F. Scott, J. Phys. Condens. Matter **18**, R361 (2006).
[36]G. Catalan, H. Bea, S. Fusil, M. Bibes, P. Paruch, A. Barthelemy, and J. F. Scott, Phys. Rev. Lett. **100**, 027602 (2008).
[37]I. Horcas, R. Fernandez, J. M. Gomez-Rodriguez, J. Colchero, J. Gomez-Herrero, and A. M. Baro, Rev. Sci. Instrum. **78**, 013705 (2007).
[38]P. Sharma, T. Nakajima, S. Okamura, and A. Gruverman, Nanotechnology **24**, 015706 (2013).
[39]P. Sharma, T. J. Reece, S. Ducharme, and A. Gruverman, Nano Lett. **11**, 1970 (2011).
[40]Z. Xiao, S. Poddar, S. Ducharme, and X. Hong, Appl. Phys. Lett. **103**, 112903 (2013).